Studies on the Synthetic System of V/Ag/S Cluster Compounds and Structural Characterizations of V_2AgS_4, $V_2Ag_2S_4$, and $V_2O_2(\mu\text{-}S)_2$ Complexes

Hongping Zhu, Qiutian Liu,* Xiaoying Huang, Tingbin Wen, Changneng Chen, and Daxu Wu

State Key Laboratory of Structural Chemistry, Fujian Institute of Research on the Structure of Matter, Chinese Academy of Sciences, Fuzhou, Fujian 350002, China

Received December 5, 1997

The reaction system $(NH_4)_3VS_4/Ag(PPh_3)_2Cl/R_2dtcNa$ in CH_3CN was studied to afford two $V_2Ag_{1-2}S_4$ cubanelike cluster compounds and a trinuclear $V_3O_3S_2$ complex. $(Et_4N)[V_2AgS_4(Me_2dtc)_2(PPh_3)]\cdot{}^1/_2CH_3CN$ ([Et4N]**1**·$^1/_2$-CH_3CN) crystallizes in the monoclinic space group $P2_1/c$ with $a = 10.525(3)$ Å, $b = 16.340(8)$ Å, $c = 26.834(8)$ Å, $\beta = 101.28(2)°$, and $Z = 4$. Complex $(Et_4N)_2[V_2Ag_2S_4(CS_3)_2(PPh_3)_2]$ ([Et4N]$_2$**2**) crystallizes in the monoclinic space group $C2/c$ with $a = 21.212(5)$ Å, $b = 20.100(4)$ Å, $c = 15.039(2)$ Å, $\beta = 102.72(2)°$, and $Z = 4$. A stepwise aggregate process including a dinuclear $V_2Y_2(\mu\text{-}S)_2$ (Y = S, O) intermediate was suggested to explain the formation of **1**, **2**, and trinuclear anion $[V_3O(\mu\text{-}O)_2(\mu\text{-}S)_2(Et_2dtc)_3]^-$. Structural features of these complexes show that the $V_2Y_2(\mu\text{-}S)_2$ moiety can be seen as an independent unit to combine with other metal ion(s). A complex containing the $[V_2O_2(\mu\text{-}S)_2(Et_2dtc)_2]^{2-}$ (**3**) cluster anion was separated from a reaction system of $(NH_4)_3$-$VS_4/PPh_3/Et_2dtcNa$, and its solvate complex $\{(Et_4N)_3Na[V_2O_2(\mu\text{-}S)_2(Et_2dtc)_2]_2\}_2\cdot{}^1/_2CH_3OH\cdot H_2O$ crystallizes in orthorhombic space group $Pnn2$ with $a = 31.599(1)$ Å, $b = 17.228(5)$ Å, $c = 14.104(7)$ Å, and $Z = 2$. Infrared frequencies at 844−970 cm^{-1} were associated with a V═O stretching vibration. The V═O additional coordination to the other metal ion gives rise to the red shift of the frequency. Proton and ^{51}V NMR spectra exhibit a paramagnetic V^{IV} center existing in the trinuclear complex $(Et_4N)[V_3O(\mu\text{-}O)_2(\mu\text{-}S)_2(Et_2dtc)_3]$ ([Et4N]**4**) and d^1-d^1 coupling of V−V of the $V_2Y_2(\mu\text{-}S)_2$ moiety for these complexes. Two sets of the ^{31}P signals for **2** at 16.6−19.3 ppm with equal intensity are attributed to $^{31}P-^{107}Ag$ coupling and may well hide two V atoms in a similar environment. Cyclic voltammetries show some similar electrochemical behaviors between **3** and **4** indicated by a common couple at −0.7 V/−0.65 V and an oxidation peak at +0.7 to +0.6 V which are proposed to be due to redox in the $V_2O_2(\mu\text{-}S)_2$ moiety.

Introduction

Research interest in V/S and V/O chemistry derives from its relevance to several biological[1] and industrial[2] processes. Vanadium is an essential element in biological systems, taking part in some enzymic reactions, such as nitrogen fixation.[1b,c] Its insulinomimetic properties[1d] in the therapeutics of diabetes by using oxovanadium species have attracted more attention. Vanadium sulfide complexes are considered to be likely intermediates during hydrodemetalation and hydrodesulfurization in the processing[3] of crude oil. Vanadium chemistry has had an impressive advance[4−17] and is proving sufficiently different from the corresponding Mo chemistry, despite that the former is usually seen as an extension of the latter. Our interest in this area concentrates on the riches of structure types of the V/S(O) complexes and studies on synthetic systems and clustering mechanisms. We have synthesized and structurally

* To whom correspondence should be addressed.

(1) (a) Rehder, D. *Angew. Chem., Int. Ed. Engl.* **1991**, *30*, 148. (b) Chisnell, J. R.; Premakumar, R.; Bishop, P. E. *J. Bacteriol.* **1988**, *170*, 27. (c) Hales, B. T.; Case, E. E.; Morningstar, J. E.; Dzeda, M. F.; Mauterer, L. A. *Biochemistry* **1986**, *25*, 7251. (d) Butler, A.; Walker, J. V. *Chem. Rev.* **1993**, *93*, 1937. (e) Butler, A.; Clague, M. J.; Meister, G. E. *Chem. Rev.* **1994**, *94*, 625.

(2) (a) Rouxel, J.; Brec, R. *Annu. Rev. Mater. Sci.* **1986**, *16*, 137. (b) Reynolds, J. F.; Biggs, W. R.; Fetzer, J. C. *Liq. Fuel Technol.* **1985**, *3*, 423. (c) Nakajima, K.; Kojima, K.; Kojima, M.; Fujita, J. *Bull. Chem. Soc. Jpn.* **1990**, *63*, 2620. (d) Nakajima, K.; Kojima, M.; Toriumi, K.; Saito, K.; Fujita, J. *Bull. Chem. Soc. Jpn.* **1989**, *62*, 760.

(3) (a) Silbernagel, B. G. *J. Catal.* **1979**, *56*, 315. (b) Rosa-Brussin, M.; Moranta, D. *Appl. Catal.* **1984**, *11*, 85. (c) Mitchell, P. C. H.; Scott, C. E.; Bonnelle, J.-P.; Grimblot, J. G. *J. Chem. Soc., Faraday Trans. 1* **1985**, *81*, 1047.

(4) (a) Holm, R. H. *Adv. Inorg. Chem.* **1992**, *38*, 1. (b) Cen, W.; Lee, S. C.; Li, J.; MacDonnell, F. M.; Holm, R. H. *J. Am. Chem. Soc.* **1993**, *115*, 9515. (c) Nordlander, E.; Lee, S. C.; Cen, W.; Wu, Z. Y.; Natoli, C. R.; Cicco, A. D.; Filipponi, A.; Hedman, B.; Hodgson, K. O.; Holm, R. H. *J. Am. Chem. Soc.* **1993**, *115*, 5549. (d) Cen, W.; MacDonnell, F. M.; Scott, M. J.; Holm, R. H. *Inorg. Chem.* **1994**, *33*, 5809. (e) Huang, J.; Mukerjee, S.; Segal, B. M.; Akashi, H.; Zhou, J.; Holm, R. H. *J. Am. Chem. Soc.* **1997**, *119*, 8662.

(5) (a) Castro, S. L.; Streib, W. E.; Sun, J.-S.; Christou, G. *Inorg. Chem.* **1996**, *35*, 4462. (b) Reynold, J. G.; Sendlinger, S. C.; Murray, A. M.; Huffman, J. C.; Christou, G. *Inorg. Chem.* **1995**, *34*, 5745. (c) Dean, N. S.; Bartley, S. L.; Streib, W. E.; Lobkovsky, E. B.; Christou, G. *Inorg. Chem.* **1995**, *34*, 1608. (d) York, K. A.; Folting, K.; Christou, G. *J. Chem. Soc., Chem. Commun.* **1993**, 1563. (e) Dean, N. S.; Folting, K.; Lobkovsky, E. B.; Christou, G. *Angew. Chem., Int. Ed. Engl.* **1993**, *32*, 594. (f) Castro, S. L.; Martin, J. D.; Christou, G. *Inorg. Chem.* **1993**, *32*, 2978. (g) Money, J. K.; Huffman, J. C.; Christou, G. *Inorg. Chem.* **1988**, *27*, 507. (h) Money, J. K.; Huffman, J. C.; Christou, G. *J. Am. Chem. Soc.* **1987**, *109*, 2210. (i) Money, J. K.; Nicholson, J. R.; Huffman, J. C.; Christou, G. *Inorg. Chem.* **1986**, *25*, 4072.

(6) (a) Cotton, F. A.; Lewis, G. E.; Mott, G. N. *Inorg. Chem.* **1982**, *21*, 3316. (b) Cotton, F. A.; Extine, M. W.; Falvello, L. R.; Lewis, D. B.; Lewis, G. E.; Murillo, C. A.; Schwotzer, W.; Tomas, M.; Troup, J. M. *Inorg. Chem.* **1986**, *25*, 3505.

(7) (a) Lin, F.; Beddoes, R. L.; Collison, D.; Garner, C. D.; Mabbs, F. E. *J. Chem. Soc., Chem. Commun.* **1993**, 496. (b) Scattergood, C. D.; Bonney, D. G.; Slater, J.; Garner, C. D.; Clegg, W. *J. Chem. Soc., Chem. Commun.* **1987**, 1749.

S0020-1669(97)01531-0 CCC: $15.00
Published on Web 05/06/1998

characterized several V/S complexes, such as $V_2(\eta^2\text{-}\mu\text{-}S_2)_2(Et_2dtc)_4$,[18] $[V_3S_7(Me_2dtc)_3]^-$,[19] $[V_2Cu_2S_4(R_2dtc)_2(PhS)_2]^{2-}$ (R_2 = Me_2,[20] C_5H_{10},[21] and OC_4H_8),[22] $[V_2Fe_2S_4(Me_2dtc)_5]^-$,[23] $[VFe_3S_4(Et_2dtc)_4]^-$,[24] $[V_2Ag_2S_4(OC_4H_8dtc)_2(PhS)_2]^{2-}$,[22] and $[VS_4Cu_4(R_2dtc)_n(PhS)_{4-n}]^{3-}$ ($R_2 = OC_4H_8$, $n = 0, 1, 2$; $R_2 = Et_2$, $n = 1$).[25] All the above complexes were obtained in this laboratory from an assembly system consisting of VS_4^{3-}, M^{n+} (M = Fe, Cu, Ag), and R_2dtc^- and/or PhS^-. As a unique example, the $V_2Ag_2S_4$ cubanelike complex $(Et_4N)_2[V_2Ag_2S_4(OC_4H_8dtc)_2(PhS)_2]$ was obtained in very low yield (less than 1%) from the synthetic system of $VS_4^{3-}/Ag(PPh_3)_2^+/OC_4H_8dtc^-/PhS^-$. A possible intermediate possessing the $V_2Y_2(\mu\text{-}S)_2$ (Y = O, S) structural unit has been considered to construct cluster skeletons of polynuclear or heteronuclear V/O or V/S complexes according to studies on $M_2M'_{1-2}S_4$ (M = Mo, W; M′ = Cu, Ag) cubanelike clusters[26] and $[V_3O_3S_2(Et_2dtc)_3]^-$ complexes.[7a] However, the dinuclear $V_2Y_2(\mu\text{-}S)_2$ complex has not yet been synthesized although the corresponding molybdenum analogues, $Mo_2Y_2(\mu\text{-}S)_2$, are well-known.[27] This paper report further study on the V/Ag/S synthetic system, in which two novel cubanelike cluster compounds have been obtained. Also included is the first example of a dinuclear $V_2O_2(\mu\text{-}S)_2$ complex, $(Et_4N)_3Na[V_2O_2(\mu\text{-}S)_2(Et_2dtc)_2]_2$.

Experimental Section

All manipulations were carried out under a dinitrogen atmosphere, and a Schlenk apparatus was used throughout the experimental process. The solvents were dried with molecular sieves and degassed prior to use. Compounds $(NH_4)_3VS_4$[28] and $Ag(PPh_3)_2Cl$[29] were prepared by literature methods. Sodium dialkyldithiocarbamates (R_2dtcNa, R = Me; RR′dtcNa, R = Ph, R′ = Me) were prepared in good yield by reaction of equimolar amounts of dialkylamine, NaOH, and CS_2 in aqueous solution at about 5−10 °C as previously described.[30] Sodium cyclopentanethiolate was prepared by reaction of equimolar amounts of C_5H_9SH and Na in THF. Reagents $Et_2dtcNa\cdot 3H_2O$, Et_4NCl, and PPh_3 were commercially available and used without further purification.

$(Et_4N)[V_2AgS_4(Me_2dtc)_2(PPh_3)]$ ([Et$_4$N]1). In 50 mL of CH_3CN, 0.233 g (1.0 mmol) of $(NH_4)_3VS_4$, 1.336 g (2.0 mmol) of $Ag(PPh_3)_2Cl$, 0.573 g (4.0 mmol) of Me_2dtcNa, and 0.397 g (2.4 mmol) of Et_4NCl were mixed and stirred for 24 h at room temperature, giving rise to a change of solution color from dark-green to red-brown. After filtration, large amounts of black intractable precipitates were removed and the filtrate was allowed to stand at room temperature for several days, to give 0.02 g of black stick crystals mixed in with a few powdery impurities. The crystals were picked out and were identified to be $(Et_4N)[V_2AgS_4(Me_2dtc)_2(PPh_3)]\cdot{}^1/_2CH_3CN$ by X-ray crystallography. IR (KBr, cm^{-1}): 342 (V−S_t), 455 (V−S_b), 492 (P−C), 980 (C═S, Me_2dtc), 1510 (C−N, Me_2dtc).

$(Et_4N)_2[V_2Ag_2S_4(CS_3)_2(PPh_3)_2]$ ([Et$_4$N]$_2$2). In 60 mL of CH_3CN, 0.233 g (1.0 mmol) of $(NH_4)_3VS_4$, 1.336 g (2.0 mmol) of $Ag(PPh_3)_2Cl$, 0.821 g (4.0 mmol) of sodium methylphenyldithiocarbamate, 0.496 g (4.0 mmol) of C_5H_9SNa, and 0.397 g (2.4 mmol) of Et_4NCl were mixed and stirred for 24 h at room temperature, giving rise to a change of solution color from dark-green to brown. After filtration, 20 mL of Me_2CO was added to the filtrate. The solution was allowed to stand for several days, resulting in black crystals which were collected, washed with Me_2CO, and dried in vacuo, affording 0.4 g (yield 55.3%) of product. Anal. Calcd for $C_{54}H_{70}Ag_2N_2P_2S_{10}V_2$: C, 47.30; H, 4.88; Ag, 14.91; N, 1.94; S, 22.15; V, 7.03. Found: C, 47.82; H, 4.87; Ag, 13.4; N, 2.47; S, 22.03; V, 6.00. IR (KBr, cm^{-1}): 350 (V−S_t), 430, 470 (V−S_b), 492 (P−C), 1000 (C═S, CS_3). ^{1}H NMR (DMSO-d_6, ppm): δ 1.16 (CH_3, Et_4N), 3.22 (CH_2, Et_4N), 7.56−7.69 (C_6H_5, PPh_3). ^{13}C NMR (DMSO-d_6, ppm): δ 7.28 (CH_3, Et_4N), 51.84 (CH_2, Et_4N), 128.9−132.4 (C_6H_5, PPh_3), 133.1 (P−C). ^{31}P (DMSO-d_6, ppm): δ 16.6, 16.8; 19.1, 19.3. ^{51}V NMR (DMSO, ppm): δ 231.

$(Et_4N)_3Na[V_2O_2(\mu\text{-}S)_2(Et_2dtc)_2]_2$ ([Et$_4$N]$_3$Na[3]$_2$). In 35 mL of CH_3CN, 0.233 g (1.0 mmol) of $(NH_4)_3VS_4$, 0.526 g (2.0 mmol) of PPh_3, 0.691 g (3.1 mmol) of $Et_2dtcNa\cdot 3H_2O$, and 0.397 g (2.4 mmol) of Et_4NCl were mixed and stirred for 24 h. After filtration, the filtrate with brown-red color was concentrated in vacuo to reduce the volume to 25 mL. On standing for 2 days at room temperature, light colored microcrystals deposited and were removed by filtration. The filtrate was allowed to stand for several days resulting in the separation of black square crystals, which were collected and dried in a vacuum to give 0.28 g (yield 79.8%) of product. Anal. Calcd for $C_{44}H_{100}N_7NaO_4S_{12}V_4$: C, 37.67; H, 7.18; N, 6.99. Found: C, 36.34; H, 7.23; N, 6.93. IR (KBr, cm^{-1}): 366 (V−S_t), 467 (V−S_b), 939 (V═O), 999 (C═S, Et_2dtc), 1489 (C−N, Et_2dtc). ^{1}H NMR (DMSO-d_6, ppm): δ 1.06 (CH_3, Et_2dtc), 1.15 (CH_3, Et_4N), 3.20 (CH_2, Et_4N), 3.97 (CH_2, Et_2dtc). ^{51}V NMR (DMSO-d_6, ppm): δ −390.

$(Et_4N)[V_3O(\mu\text{-}O)_2(\mu\text{-}S)_2(Et_2dtc)_3]\cdot{}^1/_2CH_3CN$ ([Et$_4$N]4$\cdot{}^1/_2$CH$_3$CN) and $V(Et_2dtc)_3$ (5). Complex $[Et_4N]\mathbf{4}\cdot 1.5H_2O$ was synthesized by reacting VCl_3, Li_2S, Et_4NBr, and $Et_2dtcNa\cdot 3H_2O$, and its crystal structure was reported.[7a] Here a reaction originally carried out with the intention of synthesizing a heterometallic V/Ag/S complex unexpectedly resulted in **4** and **5**. A mixture of $(NH_4)_3VS_4$ (0.23 g, 1.0 mmol), $Ag(PPh_3)_2Cl$ (1.34 g, 2.0 mmol), $Et_2dtcNa\cdot 3H_2O$ (1.00 g, 4.4 mmol), and Et_4NCl (0.40 g, 2.4 mmol) in 35 mL of CH_3CN was stirred for 24 h. After filtration the filtrate was allowed to stand for several

(8) Müller, A.; Schimanski, J.; Bögge, H. *Z. Anorg. Allg. Chem.* **1987**, *154*, 107.
(9) Yu, X.; Zheng, F.; Huang, L. *Polyhedron* **1995**, *14*, 3599.
(10) Halbert, T. R.; Hutchings, L. L.; Rhodes, R. Stiefel, E. I. *J. Am. Chem. Soc.* **1986**, *108*, 6437.
(11) Klich, P. R.; Daniher, A. T.; Challe, P. R.; McConville, D. B.; Youngs, W. J. *Inorg. Chem.* **1996**, *35*, 347.
(12) (a) Tsagkalidis, W.; Rodewald, W.; Rehder, D. *J. Chem. Soc., Chem. Commun.* **1995**, *2*, 165. (b) Tsagkalidis, W.; Rodewald, W.; Rehder, D. *Inorg. Chem.* **1995**, *34*, 1943.
(13) Kawaguchi, H.; Tatsumi, K.; Nakamura, A. *J. Chem. Soc., Chem. Commun.* **1995**, 111.
(14) (a) Rauchfuss, T. B.; Weatherill, T. D.; Wilson, S. R.; Zebrowski J. P. *J. Am. Chem. Soc.* **1983,** *105*, 6508. (b) Bolinger, C. M.; Weatherill, T. D.; Rauchfuss, T. B.; Rheingold, A. L.; Day, C. S.; Wilson, S. R. *Inorg. Chem.* **1986**, *25*, 634. (c) Bolinger, C. M.; Rauchfuss, T. B.; Rheingold, A. L. *J. Am. Chem. Soc.* **1983,** *105*, 6321.
(15) Durij, S. A.; Andras, M. T.; Kibala, P. A. *Inorg. Chem.* **1990**, *29*, 1232.
(16) Nanda, K. K.; Sinn, E.; Addison, A. W. *Inorg. Chem.* **1996**, *35*, 1.
(17) Szeymies, D.; Kebs, B.; Henkel, G. *Angew. Chem., Int. Ed. Engl.* **1983**, *22*, 885.
(18) Yang, Y.; Huang, L.; Liu, Q.; Kang, B. *Acta Crystallogr.* **1991**, *C47*, 2085.
(19) Yang, Y.; Liu, Q.; Wu, D. *Inorg. Chim. Acta* **1993**, *208*, 85.
(20) Yang, Y.; Liu, Q. *Acta Crystallogr.* **1993**, *C49*, 1623.
(21) Liu, Q.; Yang, Y.; Huang, L.; Wu, D.; Kang, B.; Ghen, C.; Deng, Y.; Lu, J. *Sci. Chi.* **1995**, *B38*, 1425.
(22) Yang, Y.; Liu, Q.; Huang, L.; Kang, B.; Lu, J. *J. Chem. Soc., Chem. Commun.* **1992**, 1512.
(23) Deng, Y.; Liu, Q.; Yang, Y.; Wang, Y.; Cai, Y.; Wu, D.; Chen, C.; Kang, B.; Liao, D.; Lu, J. *Inorg. Chem.* **1997**, *36*, 214.
(24) Deng, Y.; Liu, Q.; Wang, Y.; Cai, Y.; Wu, D.; Chen, C.; Kang, B.; Liao, D.; Cui, J. *Polyhedron* **1997**, *16*, 4121.
(25) Liu, Q.; Yang, Y.; Huang, L.; Wu, D.; Kang, B.; Chen, C.; Deng, Y.; Lu, J. *Inorg. Chem.* **1995**, *34*, 1884.
(26) (a) Zhu, N.; Zheng, Y.; Wu, X. *Inorg. Chem.* **1990**, *29*, 2707. (b) Zhu, N.; Wu, X.; Lu, J. *J. Chem. Soc., Chem. Commun.* **1991**, *23*5. (c) Zhu, N.; Zheng, Y.; Wu, X. *J. Chem. Soc., Chem. Commun.* **1990**, 780. (d) Chen, H.; Lu, S.; Huang, J.; Wu, Q.; Huang, X. *Acta Chim. Sin.* **1994**, *52*, 1088. (e)Yu, R.; Lu, S.; Huang, X.; Huang, J. *Jiegou Huaxue (Chin. J. Struct. Chem.)* **1996**, *15*, 347.
(27) (a) Howlader, N. C.; Haight, G. P., Jr.; Hambley, T. W.; Snow, M. R.; Lawrance, G. A. *Inorg. Chem.* **1984**, *23*, 1811. (b) Schultz, F. A.; Ott, V. R.; Rolison, D. S.; Bravard, D. C.; McDonald, J. W.; Newton, W. E. *Inorg. Chem.* **1978**, *17*, 1758. (c) Garner, C. D.; Charnock, J. M. In *Comprehensive Coordination Chemistry*; Wilkinson, G., Gillar, R. D., McCleverty, J. A., Eds.; Pergamon Press: Oxford, U.K., 1987; Vol. 3, p 1358. (d) Lu, S.; Huang, J.; Chen, H.; Wu, Q. *Acta Chim. Sin.* **1993**, *51*, 885.
(28) Do, Y.; Simhon, E. D.; Holm, R. H. *Inorg. Chem.* **1985**, *24*, 4635.
(29) Muetterties, E. L.; Alegranti, C. W. *J. Am. Chem. Soc.* **1972**, *94*, 6386.
(30) Bhat, A. N.; Fay, R. C.; Lewis, D. F.; Lindmark, A. F.; Strauss, S. H. *Inorg. Chem.* **1974**, *13*, 886.

Table 1. Crystallographic Data for Three Compounds[a] Containing the **1**, **2**, or **3** Anion

chem formula	$C_{33}H_{48.5}AgN_{3.5}PS_8V_2$[b]	$C_{54}H_{70}Ag_2N_2P_2S_{10}V_2$[c]	$C_{88.5}H_{204}N_{14}Na_2O_{9.5}S_{24}V_8$[d]
fw	991.47	1447.33	2839.824
space group	$P2_1/c$ (No. 14)	$C2/c$ (No. 15)	$Pnn2$ (No. 34)
a, Å	10.525(3)	21.212(5)	31.599(3)
b, Å	16.340(8)	20.100(4)	17.228(5)
c, Å	26.834(8)	15.039(2)	14.104(7)
β, deg	101.28(2)	102.72(2)	
V, Å^3	4526(3)	6255(2)	7677.9
Z	4	4	2
T, °C	23	23	23
λ, Å	0.710 73	0.710 73	0.710 73
ρ_{calcd}, g/cm^3	1.45	1.54	1.70
μ, cm^{-1}	12.3	12.99	13.9
R[e]	0.058	0.039	0.073
R_w[f]	0.068	0.056	0.077

[a] For complex $(Et_4N)[V_3O_3(\mu\text{-}S)_2(Et_2dtc)_3]\cdot{}^1/_2MeCN$, see ref 32. [b] $(Et_4N)[V_2AgS_4(Me_2dtc)_2(PPh_3)]\cdot{}^1/_2CH_3CN$. [c] $(Et_4N)_2[V_2Ag_2S_4(CS_3)_2(PPh_3)_2]$. [d] $\{(Et_4N)_3Na[V_2O_2(\mu\text{-}S)_2(Et_2dtc)_2]_2\}_2\cdot H_2O\cdot{}^1/_2CH_3OH$. [e] $R = \sum|F_o - F_c|/\sum F_o$. [f] $R_w = [\sum w(F_o - F_c)^2/\sum wF_o^2]^{1/2}$.

days at room temperature, causing the separation of red-brown crystals, which were collected and were identified to be $V(Et_2dtc)_3$ by X-ray diffraction.[31] Yield: 0.12 g (24.2%). Anal. Calcd for $C_{15}H_{30}N_3S_6V$: C, 36.34; H, 6.10; N, 8.48; S, 38.81; V, 10.28. Found: C, 36.60; H, 6.14; N, 8.49; S, 37.71; V, 10.09. IR (KBr, cm^{-1}): 364 (V−S$_t$), 997 (C═S, Et_2dtc), 1495 (C−N, Et_2dtc).

The filtrate from which **5** was collected was concentrated in vacuo to reduce the volume to 20 mL and then was filtered to remove the precipitates. After the filtrate was let to stand for several days, black square crystals were deposited and were collected yielding 0.15 g (52.3%) of complex $[Et_4N]\mathbf{4}\cdot{}^1/_2CH_3CN$.[32] Anal. Calcd for $C_{24}H_{51.5}N_{4.5}O_3S_8V_3$: C, 33.49; H, 6.03; N, 7.33; S, 29.81; V, 17.76. Found: C, 33.94; H, 6.12; N, 7.85; S, 30.87; V, 16.87. IR (KBr, cm^{-1}): 369 (V−S$_t$), 450, 487 (V−S$_b$), 844 (V═O−V), 970 (V═O), 996 (C═S, Et_2dtc), 1492 (C−N, Et_2dtc). ^{1}H NMR (DMSO-d_6, ppm): δ 1.08 (CH_3, Et_4N and Et_2dtc), 3.10 (CH_2, Et_4N^+), 9.75 (CH_2, Et_2dtcVO_3). ^{51}V NMR (DMF, ppm): δ −385, −519.

X-ray Crystallography and Structure Solution. a. Data Collection and Reduction. Single crystals of compounds $[Et_4N]\mathbf{1}\cdot{}^1/_2CH_3CN$ and $[Et_4N]_2\mathbf{2}$ were selected directly from the respective reaction solution. Solvent-free complex $[Et_4N]_3Na[\mathbf{3}]_2$ obtained in a vacuum was not suitable for X-ray diffraction and was recrystallized from CH_3CN/CH_3OH to give the suitable single crystals containing solvents of crystallization. A single crystal carefully chosen for each compound was coated with epoxy resin and mounted on a glass fiber. Data were collected at 23 ± 1 °C on an Enraf-Nonius CAD4 diffractometer equipped with a graphite crystal monochromator using the $\omega-2\theta$ scan technique. For the crystals of $[Et_4N]\mathbf{1}\cdot{}^1/_2CH_3CN$, $[Et_4N]_2\mathbf{2}$, and the solvate complex of **3**, $\{(Et_4N)_3Na[\mathbf{3}]_2\}_2\cdot H_2O\cdot{}^1/_2CH_3OH$, 8330, 5672, and 7439 independent reflections were obtained, respectively. *LP* corrections and empirical absorption corrections based on a series of ψ-scans were applied to the data. After structure refinement with isotropic thermal parameters, an empirical absorption correction using the DIFABS program[33] was made for the third complex. Crystal parameters are listed in Table 1.

b. Structure Solution and Refinement. The structures were solved by direct methods for complexes $[Et_4N]\mathbf{1}\cdot{}^1/_2CH_3CN$ and $\{(Et_4N)_3Na[\mathbf{3}]_2\}_2\cdot H_2O\cdot{}^1/_2CH_3OH$ and by heavy atom method for complex $[Et_4N]_2\mathbf{2}$. The major atoms were located from an *E*-map. Subsequent difference Fourier calculations revealed the positions of the remaining non-hydrogen atoms. All non-hydrogen atoms in these complexes were refined anisotropically by full-matrix least-squares methods except the oxygen atom of the solvent H_2O of complex **3**, which was isotropically refined. A solvent molecule CH_3CN in $[Et_4N]\mathbf{1}\cdot{}^1/_2CH_3CN$ was located at its position with occupancy of 0.5. Complex $[Et_4N]_2\mathbf{2}$ contains a carbon atom C(7) belonging to a Et_4N cation, which was found to be disordered over two positions with equal occupancies. All hydrogen atoms in these complexes were geometrically located and added to the structure factor calculations, but their positions were not refined. It is necessary to explain that the structure of complex **3** was first tried to be solved in space group *Pnnm* but the treatment was unsuccessful using either direct methods or the heavy atom method, so that the space group *Pnn*2 of lower symmetry was used to obtain the present results. Even so, a further effort using the present positional parameters to make a search for a symmetrical center and to solve the structure in *Pnnm* again was performed but also failed. The final cycles of refinements included 451, 335, and 663 variable parameters for 4988, 4778, and 4860 reflections with $I > 3\sigma(I)$ for complexes $[Et_4N]\mathbf{1}\cdot{}^1/_2CH_3CN$, $[Et_4N]_2\mathbf{2}$, and $\{(Et_4N)_3Na[\mathbf{3}]_2\}_2\cdot H_2O\cdot{}^1/_2CH_3OH$, respectively. The highest peaks in the respective difference Fourier maps were 0.97 and −0.72 e/Å^3 for $[Et_4N]\mathbf{1}\cdot{}^1/_2CH_3CN$, 0.54 and −0.98 e/Å^3 for $[Et_4N]_2\mathbf{2}$, and 0.62 and −0.10 e/Å^3 for $\{(Et_4N)_3Na[\mathbf{3}]_2\}_2\cdot H_2O\cdot{}^1/_2CH_3OH$. All calculations were performed on a COMPAQ computer using the MolEN/PC program.[34]

Other Physical Measurements. Infrared spectra were recorded on an FTS-40 spectrophotometer (Bio-Rad Co.). NMR spectra were recorded on a Bruker-AM 500 spectrometer with Me_4Si as standard for ^{1}H, H_3PO_4 for ^{31}P, and $VOCl_3$ for ^{51}V, respectively. Electrochemical measurements were performed in the cyclic voltammetric mode on a CV-1B cyclic voltammeter (Bioanalytical Systems Inc.) with an SCE reference electrode, Pt plate working electrode, and Pt auxiliary electrode. The supporting electrolyte was Bu_4NClO_4.

Results and Discussion

Synthesis. A procedure that seemed a passable route to the V/Ag/S heterometallic complexes was to separate the products in the assembly system of $VS_4^{3-}/Ag(PPh_3)_2^+/R_2dtc^-$ (and RS^-) according to the studies on the V/Cu/S heterometallic complexes $(Et_4N)_2[V_2Cu_2S_4(R_2dtc)_2(PhS)_2]$[21,22] and $(Et_4N)_3[VS_4Cu_4(R_2dtc)_n(PhS)_{4-n}]$.[25] This approach proved successful by the separation of a series of V/Ag/S complexes, $[Et_4N]\mathbf{1}$, $[Et_4N]_2\mathbf{2}$, and $(Et_4N)_2[V_2Ag_2S_4(OC_4H_8dtc)_2(PhS)_2]$,[22] though the yields of **1** complex and the third complex were very low. However, an unexpected trinuclear V_3 monoanion **4** was also obtained, implying dinuclear intermediate $[V_2Y_2(\mu\text{-}S)_2(R_2dtc)_2]^{2-}$ (**3**, Y

(31) Zhu, H.; Deng, Y.; Huang, X.; Chen, C.; Liu, Q. *Acta Crystallogr.* **1997**, *C53*, 692.

(32) $(Et_4N)[V_3O(\mu\text{-}O)_2(\mu\text{-}S)_2(Et_2dtc)_3]\cdot{}^1/_2CH_3CN$ has almost the same crystal structure parameters and structural features as $(Et_4N)[V_3O(\mu\text{-}O)_2(\mu\text{-}S)_2(Et_2dtc)_3]\cdot 1.5H_2O$ except for the solvate molecule. $\mathbf{4}\cdot{}^1/_2CH_3CN$ crystallizes in the monoclinic space group $C2/c$ (No. 15), with a = 26.472(3) Å, b = 16.001(3) Å, c = 23.761(2) Å, β = 124.73(1)°, V = 8271.0 Å^3, and Z = 8. The structure was solved by direct methods followed by successive difference Fourier syntheses from 5439 reflections with $F_o^2 > 3.0\sigma(F_o^2)$ and refined to R (R_w) = 0.048 (0.070). An ORTEP figure is shown in Figure 4, and some bond distances and angles are listed in Table 6 for comparison.

(33) Walker, N.; Stuart, D. *Acta Crystallogr.* **1983**, *A39*, 159.

(34) MolEN, *An Interactive Structure Solution Procedure*, Enraf-Nonius: Delft, The Netherlands, 1990.

Scheme 1. Aggregation of Vanadium-Containing Species in the Reaction System

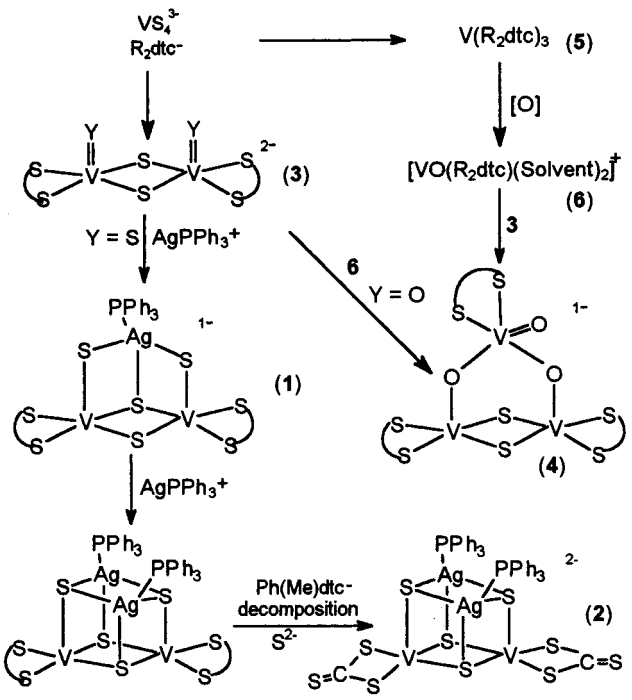

= S, O) and an exchange of S/O existing in the reaction system. The reaction pathways of Scheme 1 are suggested.

It is noted that the V^V in VS_4^{3-} is reduced to V^{IV} in these polynuclear V/Ag/S or V/O/S complexes and to V^{III} in $V(Et_2dtc)_3$. Phosphine, dithiocarbamate and/or thiolate are believed to play the role of reducing agent to reduce VS_4^{3-}. It is also believed that permeation of a little air and the participation of solvate H_2O from the $Et_2dtcNa{\cdot}3H_2O$ salt result in the formation of VO−dithiocarbamate species, such as $VO(Et_2dtc)_2$ and $[V_2O_2(\mu\text{-}S)_2(Et_2dtc)_2]^{2-}$, of which the former was found in the conversion[35] of $V(Et_2dtc)_3$ and the latter may come from the O/S exchange of $[V_2S_2(\mu\text{-}S)_2(R_2dtc)_2]^{2-}$, a possible but not exclusive intermediate, in the aggregation mechanism forming $V_2Ag_{1-2}S_4$ cubanes. In another assembly system of $VS_4^{3-}/PPh_3/Et_2dtc^-$ we have obtained $[V_2O_2(\mu\text{-}S)_2(Et_2dtc)_2]^{2-}$, showing that the $V_2Y_2(\mu\text{-}S)_2$ intermediate exists probably in the aggregation process and that the aggregation mechanism seems to be reasonable. The analogues of the V_2AgS_4 complex, the Mo_2AgS_4 and W_2AgS_4 complexes,[26b] have been synthesized by the reactions of $(Et_4N)_2[M_2S_2(\mu\text{-}S)_2(edt)_2]$ (M = Mo, W; edt = ethanedithiolate) with $Ag(PPh_3)_3NO_3$, and meanwhile, the further aggregation of the M_2AgS_4 defective cubane (M = Mo, W) with $Ag(PPh_3)^+$ has also been reported to form $M_2Ag_2S_4$ cubanelike clusters.[26d,e] It is noteworthy that these **1**−**4** anions contain a $V_2Y_2(\mu\text{-}S)_2$ (Y = S, O) structural unit with hard and soft Lewis base donor atoms O and S, which have a tendency to coordinate to the metal ions as hard and soft Lewis acids. Consequently, the sulfur atoms in the $V_2Y_2(\mu\text{-}S)_2$ unit or in the $M_2S_2(\mu\text{-}S)_2$ (M = Mo, W) unit tend to combine with Ag ion, being a soft acid, to result in $V_2Ag_{1-2}S_4$ or $M_2Ag_{1-2}S_4$ cubanelike clusters, while the oxygen atoms compared to the S atoms in the $V_2O_2(\mu\text{-}S)_2$ unit have a greater tendency to combine V-containing group, such as $VO(R_2dtc)^+$, to give the trinuclear $V_3O(\mu\text{-}O)_2(\mu\text{-}S)_2$ cluster anion **4** without a $V_3(\mu_3\text{-}S)$ group in the molecule. It is also noted that anion **2** is the first example of a heterometallic thiocubane containing a trithiocarbonate ligand. Apparently, the CS_3^{2-} ligand is formed from decomposed $Ph(Me)dtc^-$ and S^{2-}, since to our knowledge the stability of the aromatic dtc would be lower than that of a dialkyl dtc ligand.

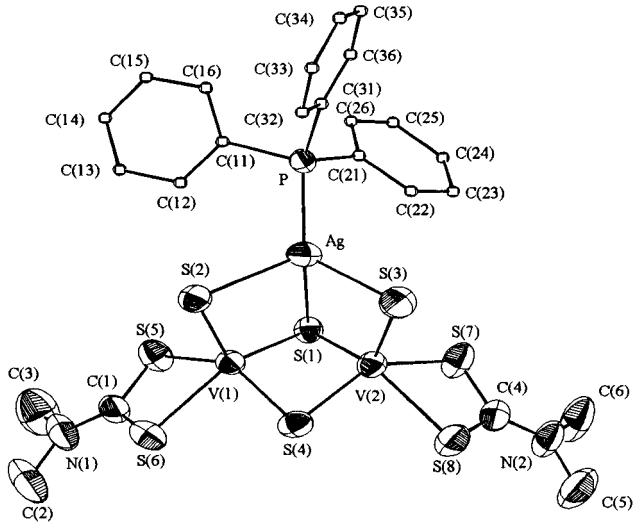

Figure 1. Structure and labeling of $[V_2AgS_4(Me_2dtc)_2(PPh_3)]^-$. Thermal ellipsoids as drawn by ORTEP represent the 30% probability surfaces. All the carbon atoms of PPh_3 are drawn as "○" for clarity.

Table 2. Selected Bond Distances (Å) and Angles (deg) for **1**

Ag−V(2)	2.947(1)	Ag−V(1)	2.978(1)
V(1)−V(2)	2.846(2)		
Ag−S(1)	2.553(2)	Ag−S(2)	2.584(2)
Ag−S(3)	2.550(2)	Ag−P	2.381(2)
V(1)−S(2)	2.109(2)	V(1)−S(4)	2.254(2)
V(1)−S(1)	2.296(2)	V(1)−S(6)	2.411(3)
V(1)−S(5)	2.463(3)	V(2)−S(3)	2.111(3)
V(2)−S(4)	2.256(3)	V(2)−S(1)	2.289(2)
V(2)−S(8)	2.452(2)	V(2)−S(7)	2.463(3)
P−Ag−S(1)	116.17(7)	S(1)−V(2)−S(8)	139.1(1)
P−Ag−S(2)	119.75(7)	S(1)−V(2)−S(7)	82.84(8)
P−Ag−S(3)	126.93(8)	S(3)−V(2)−S(1)	112.9(1)
S(1)−Ag−S(2)	90.76(6)	S(3)−V(2)−S(4)	109.2(1)
S(3)−Ag−S(1)	91.91(7)	S(3)−V(2)−S(8)	104.4(1)
S(3)−Ag−S(2)	102.61(8)	S(3)−V(2)−S(7)	106.2(1)
S(1)−V(1)−S(5)	85.43(8)	S(4)−V(2)−S(1)	98.12(9)
S(1)−V(1)−S(6)	140.4(1)	S(4)−V(2)−S(7)	140.9(1)
S(2)−V(1)−S(1)	112.2(1)	S(4)−V(2)−S(8)	84.48(9)
S(2)−V(1)−S(4)	110.4(1)	S(8)−V(2)−S(7)	70.92(8)
S(2)−V(1)−S(5)	103.2(1)	V(2)−S(1)−V(1)	76.72(7)
S(2)−V(1)−S(6)	104.3(1)	V(1)−S(4)−V(2)	78.25(8)
S(4)−V(1)−S(1)	97.96(8)	V(1)−S(1)−Ag	75.58(6)
S(4)−V(1)−S(5)	141.8(1)	V(1)−S(2)−Ag	78.06(7)
S(4)−V(1)−S(6)	82.89(9)	V(2)−S(1)−Ag	74.76(6)
S(6)−V(1)−S(5)	71.42(9)	V(2)−S(3)−Ag	77.82(7)

Structure. $(Et_4N)[V_2AgS_4(Me_2dtc)_2(PPh_3)]{\cdot}{}^1/_2CH_3CN$ ($[Et_4N]\mathbf{1}{\cdot}{}^1/_2CH_3CN$). The X-ray structure shows that the anion **1**, the cation $(Et_4N)^+$ and the solvent molecule CH_3CN are discrete units, and the latter two will not be discussed further. The molecular structure and numbering scheme for **1** are shown in Figure 1, and selected structural parameters are found in Table 2. The structure of the anion contains a defective V_2AgS_4 cubanelike core. Each vanadium atom is coordinated by three sulfido atoms and one Me_2dtc ligand binding through two sulfur atoms. The coordination geometry is a distorted square pyramid for the each vanadium which lies out of the equatorial plane toward the apical S(2) or S(3) atom with the bond angles of $S_{apical}-V-S$ ranging from 103.2(1) to 112.9(1)°. All the V−S

(35) Riechel, T. L.; de Hayes, L. J.; Sawyer, D. T. *Inorg. Chem.* **1976**, *15*, 1900.

Table 3. Comparison of Bond Distances (Å) in $M_2Ag_{1-2}S_4$ (M = Mo, W, V) Cubanelike Complexes

	M−S_{core}	Ag−S_{core}	Ag−P	V−S_{term}	ref
$[Mo_2AgS_4(edt)_2(PPh_3)]^-$	2.33(1)−2.36(1) mean 2.34(1)[a] 2.15(1)−2.16(1) mean 2.16(1)[a]	2.55(1)−2.71(1) mean 2.62(5)[a]	2.405(8)		26b
$[W_2AgS_4(edt)_2(PPh_3)]^-$	2.300(4)−2.394(4) mean 2.342(24)[a] 2.195(4)−2.200(4) mean 2.198(3)[a]	2.568(4)−2.720(5) mean 2.620(50)[a]	2.398(4)		26b
$[V_2AgS_4(Me_2dtc)_2(PPh_3)]^-$	2.254(2)−2.296(2) mean 2.274(11)[a] 2.109(2)−2.111(3) mean 2.110(1)[a]	2.550(2)−2.584(2) mean 2.562(11)[a]	2.381(2)	2.411(3)−2.463(3) mean 2.447(12)[a]	this work
$Mo_2Ag_2S_4(tdt)_2(PPh_3)_2$	2.349(2)−2.363(2) mean 2.357(3)[a] 2.182(2)−2.187(2) mean 2.185(3)[a]	2.527(2)−2.797(2) mean 2.626(52)[a]	2.382(2)	2.357(2)−2.371(2) mean 2.367(3)[a]	26d
$W_2Ag_2S_4(tdt)_2(PPh_3)_2$	2.349(2)−2.361(2) mean 2.354(3)[a] 2.188(2)−2.192(3) mean 2.190(2)[a]	2.552(3)−2.809(3) mean 2.636(51)[a]	2.381(4)	2.353(3)−2.367(3) mean 2.363(3)[a]	26e
$[V_2Ag_2S_4(OC_4H_8dtc)_2(PhS)_2]^{2-}$	2.264(5)−2.293(7) mean 2.279(15)[a] 2.138(6)	2.480(5)−2.670(5) mean 2.607(63)[a]		2.403(6)−2.450(7) mean 2.427(24)[a]	22
$[V_2Ag_2S_4(CS_3)_2(PPh_3)_2]^{2-}$	2.284(1)−2.292(1) mean 2.288(4)[a] 2.160(1)	2.541(1)−2.665(1) mean 2.601(36)[a]	2.405(1)	2.404(1)−2.409(1) mean 2.407(3)[a]	this work

[a] Number in parentheses represents the standard deviation from the mean, $\sigma = [\sum_{i=1}^{N} (x_i - \bar{x})^2/N(N-1)]$.

bonds are divided into three sets, V−S_{apical}, V−S_{bridge}, and V−S_{dtc}, of which the shortest is the first (2.109(2)−2.111(1) Å). Both the V atoms possess identical coordination environments and their corresponding structural parameters are in a fairly narrow range (Table 2), emphasizing the approach of the V_2AgS_4 core to C_s symmetry. A mirror plane including the Ag, S(1), S(4), and P atoms was found with the largest deviation of 0.059(1) Å from the least-squares plane for Ag. The silver atom has a seriously distorted tetrahedral coordination environment with the bond angles around Ag ranging from 90.76(6) to 126.93(8)°. Three metal−metal interactions are observed including two V−Ag bonds (2.947(1), 2.978(1) Å), which are shorter than those (2.998−3.038 Å) in $V_2Ag_2S_4$ cubanelike cluster anion **2** and $[V_2Ag_2S_4(OC_4H_8dtc)_2(PhS)_2]^{2-}$,[22] and one V−V bond (2.846(2) Å), which is close to those in other V^{IV} complexes[10,14c,15,18,36] and is believed to contain a V−V single bond. It appears that the structure of **1** can be seen as a combination of two moieties, $[V_2S_2(\mu\text{-}S)_2(Me_2dtc)_2]^{2-}$ and $Ag(PPh_3)^+$, by means of three Ag−S bonds and two weak V−Ag intermetallic contacts, if we notice that both the shortest V−S_{apical} bond distances are very near the V═S double bond distances (2.087(1)[37]−2.099(2)[38] Å) in 5-coordinate V/S complexes. This supports the aggregation mechanism aforementioned. Similar situations have been found in the analogues of Mo_2AgS_4 and W_2AgS_4 clusters,[26b] and their structural parameters are listed in Table 3 together with those of **1**.

Table 4. Selected Bond Distances (Å) and Angles (deg) for **2**

Ag−V	2.9984(9)	Ag−S(1)[a]	2.665(1)
Ag−V[a]	3.0862(9)	V−S(1)	2.160(1)
V−V[a]	2.835(1)	V−S(2)[a]	2.284(1)
Ag−Ag[a]	3.686(1)	V−S(2)	2.292(1)
Ag−P	2.405(1)	V−S(3)	2.404(1)
Ag−S(2)	2.541(1)	V−S(4)	2.409(1)
Ag−S(1)	2.597(1)		
S(1)−V−S(2)[a]	111.05(4)	S(2)[a]−V−S(3)	139.83(5)
S(1)−V−S(2)	113.03(4)	S(2)[a]−V−S(4)	84.44(4)
S(1)−V−S(3)	106.19(5)	S(2)−V−S(3)	82.51(4)
S(1)−V−S(4)	105.96(4)	S(2)−V−S(4)	137.68(4)
S(2)[a]−V−S(2)[a]	96.12(4)	S(3)−V−S(4)	71.17(5)
P−Ag−S(2)	114.75(4)	S(2)−Ag−S(1)	92.57(3)
P−Ag−S(1)	126.22(4)	S(2)−Ag−S(1)[a]	89.42(3)
P−Ag−S(1)[a]	132.01(4)	S(1)−Ag−S(1)[a]	90.73(4)
V−S(1)−Ag	77.54(4)	V[a]−S(2)−Ag	79.32(4)
V−S(1)−Ag[a]	78.73(4)	V−S(2)−Ag	76.49(3)
Ag−S(1)−Ag[a]	88.90(4)	V−S(2)−V[a]	76.57(4)

[a] Symmetry operator: $-x, y, {}^1/_2 - z$.

$(Et_4N)_2[V_2Ag_2S_4(CS_3)_2(PPh_3)_2]$ ($(Et_4N)_2$2). Selected bond distances and angles are listed in Table 4. An ORTEP projection of **2** is depicted in Figure 2; the structure of the Et_4N^+ cation will not be discussed further. The anion contains a $V_2Ag_2S_4$ cuboidal core. A crystallographically imposed C_2 axis passes through the middle points of both Ag−Ag′ and V−V′. Two 5-coordinate V atoms are in a distorted square-pyramidal geometry and two 4-coordinate Ag atoms are in a seriously distorted tetrahedral geometry, similar to the situations of V and Ag in **1**. Corresponding structural data for the $M_2Ag_2S_4$ (M = Mo, W, V) cubanelike complexes are compared in Table 3, indicating roughly the same structure features: (1) Except for the Ag···Ag separations (3.686(1) Å for **2**) there are obvious or weak metal−metal interactions between M and M or M and Ag. (2) There are two sets of M−S_{core} bonds in all the complexes of which two short M−S bonds display the features of a M═S double bond, indicating the relative independency of the moieties $M_2S_2(\mu\text{-}S)_2$ in the $M_2Ag_2S_4$ cores similar to that

(36) (a) Preuss, F.; Becker, H.; Kaub, J.; Sheldrick, W. S. *Z. Naturforsch* **1988**, *43B*, 1195. (b) Preuss, F.; Overhoff, G.; Becker, H.; Häusler, H. J.; Frank, W.; Reiss, G. *Z. Anorg. Allg. Chem.* **1993**, *619*, 1827. (c) Ruiz, J.; Vivanco, M.; Floriani, C.; Chiesi-Villa, A.; Guastini, C. *J. Chem. Soc., Chem. Commun.* **1991**, *214*. (d) Herberhold, M.; Kuhnlein, M.; Schrepfermann, M.; Ziegler, M. L.; Nuber, B. *J. Organomet. Chem.* **1990**, *398*, 259. (e) Duan, Z.; Schmidt, M.; Young, V. G., Jr.; Xie, X.; McCarley, R. E.; Verkade, J. G. *J. Am. Chem. Soc.* **1996**, *118*, 5302.

(37) Money, J. K.; Huffman, J. C.; Christou, G. *Inorg. Chem.* **1985**, *24*, 3297.

(38) Sendlinger, S. C.; Nicholson, J. R.; Lobkovsky, E. B.; Huffman, J. C.; Rehder, D.; Christou, G. *Inorg. Chem.* **1993**, *32*, 204.

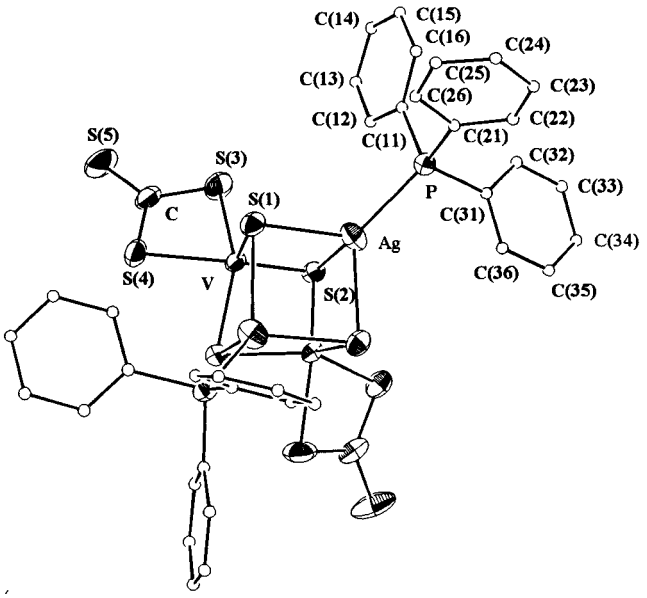

Figure 2. Structure and labeling of $[V_2Ag_2S_4(CS_3)_2(PPh_3)_2]^{2-}$. Thermal ellipsoids as drawn by ORTEP represent the 30% probability surfaces. All the carbon atoms of PPh_3 are drawn as "○" for clarity.

of the moieties in M_2AgS_4 defective cubane cores. This implies again the following aggregation mechanism:

$$[M_2S_2(\mu\text{-}S)_2]^n + Ag^+ \rightarrow [M_2Ag(\mu\text{-}S)_3(\mu_3\text{-}S)]^{n+1}$$

$$[M_2Ag(\mu\text{-}S)_3(\mu_3\text{-}S)]^{n+1} + Ag^+ \rightarrow [M_2Ag_2(\mu_3\text{-}S)_4]^{n+2}$$

In contrast with the R_2dtc^- ligand that leads usually to two unequal chelating V−S bonds,[20−24] the trithiocarbonate chelating the V atom gives two V−S bonds of almost equal length (ca. 2.406 Å). Both the $V_2Ag_2S_4$ cubanelike complexes in Table 3 show no obvious differences in core structure; their respective mixed ligands would not seem to give rise to significant variations of the cores.

$\{(Et_4N)_3Na[V_2O_2(\mu\text{-}S)_2(Et_2dtc)_2]_2\}_2\cdot{}^1/_2CH_3OH\cdot H_2O$. The X-ray crystal structure shows that there are two molecules existing in a unit cell. Two $[V_2O_2(\mu\text{-}S)_2(Et_2dtc)_2]^{2-}$ (**3**) anions are related by a 2-fold axis passing through a Na^+ cation and are linked by the Na^+ cation. An ORTEP projection including the **3** anions and Na^+ cations is depicted in Figure 3, and selected bond distances and angles are listed in Tables 5 and 6, respectively. We tried to relate two $\{Na[V_2O_2(\mu\text{-}S)_2(Et_2dtc)_2]_2\}^{3-}$ structure units through a symmetrical center but failed because of the bond angles of O−Na−O around Na(1) (96, 96, 105, 116, 116, and 124°) and Na(2) (86, 97, 97, 110, 134, and 134°) obviously being different from each other. Both the sodium ions are coordinated by four vanadyl oxygen atoms of the two related **3** anions in a distorted tetrahedral geometry with Na−O bond distances ranging from 2.29(1) to 2.33(1) Å. Each V atom in the anions has the expected square pyramidal coordination geometry with an S_4 donor set in the basal plane and an O atom in the apical position. The vanadium atoms are displaced toward the apical oxygen by 0.643−0.686 Å from the respective S_4 least-squares plane. Of the four basal S_4 planes, two planes S(1)S(2)S(5)S(6) and S(7)S(8)S(9)S(10) contain the S atoms with the largest deviation from the plane by 0.063(4) Å, while the other two have the S atoms with mean deviation of ±0.126 Å from the least-squares plane. The structural features of the $[V_2O_2(\mu\text{-}S)_2(Et_2dtc)_2]^{2-}$ moiety are compared with those of the same moiety in $(Et_4N)[V_3O(\mu\text{-}O)_2(\mu\text{-}S)_2(Et_2dtc)_3]$ ($[Et_4N]$**4**) in Table 7, and an ORTEP figure[32] of the **4** anion is also shown in Figure 4 for comparison, indicating almost identical structural parameters between the two moieties of **3** and **4** and showing that the moiety plays an important role in forming clusters. A considerable difference in V=O bond lengths for **3** (mean 1.62(1) Å) and the moiety (mean 1.677(1) Å) of **4** is due to that the formation of two V−O bonds (1.993(5) and 2.000(2) Å) between $VO(Et_2dtc)^+$ and the dinuclear moiety weakens the V=O double bonds of **4**, while the contacts between the Na^+ cation and vanadyl oxygen atoms in **3** seem not to obviously weaken the V=O bonds.

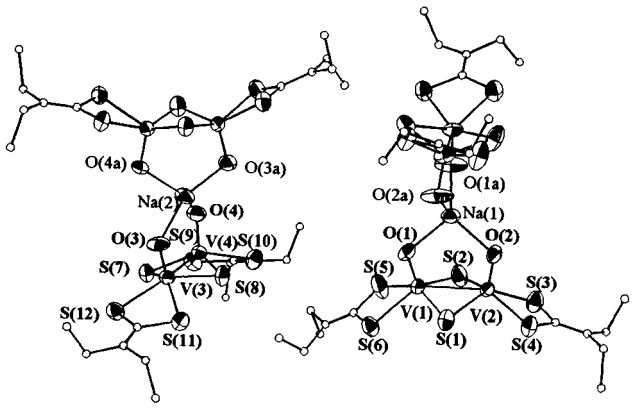

Figure 3. Structure of 2-fold axial symmetric anion and sodium ion complex of **3**. Thermal ellipsoids are drawn by ORTEP at 30% probability. A pair of such structures without their symmetric relationship are depicted. All the non-hydrogen atoms in Et_2NC groups of the ligands are drawn as "○" for clarity.

Table 5. Selected Bond Distances (Å) for **3** Including Na^+

V(1)−V(2)	2.781(4)	V(3)−V(4)	2.813(3)
V(1)−S(1)	2.285(6)	V(3)−S(7)	2.277(4)
V(1)−S(2)	2.271(6)	V(3)−S(8)	2.258(5)
V(1)−S(5)	2.478(5)	V(3)−S(11)	2.464(5)
V(1)−S(6)	2.469(5)	V(3)−S(12)	2.497(5)
V(2)−S(1)	2.273(6)	V(4)−S(7)	2.292(5)
V(2)−S(2)	2.294(6)	V(4)−S(8)	2.268(4)
V(2)−S(3)	2.438(6)	V(4)−S(9)	2.474(5)
V(2)−S(4)	2.474(5)	V(4)−S(10)	2.480(5)
V(1)−O(1)	1.63(1)	V(3)−O(3)	1.61(2)
V(2)−O(2)	1.62(1)	V(4)−O(4)	1.62(1)
Na(1)−O(1)	2.33(1)	Na(2)−O(3)	2.33(1)
Na(1)−O(2)	2.29(1)	Na(2)−O(4)	2.31(1)

Table 6. Selected Bond Angles (deg) for **3**

S(1)−V(1)−S(2)	100.4(2)	S(7)−V(3)−S(8)	100.1(2)
S(1)−V(1)−S(5)	144.7(2)	S(7)−V(3)−S(11)	139.7(2)
S(1)−V(1)−S(6)	84.4(2)	S(7)−V(3)−S(12)	86.6(2)
S(1)−V(1)−O(1)	106.7(6)	S(7)−V(3)−O(3)	109.6(4)
S(2)−V(1)−S(5)	85.7(3)	S(8)−V(3)−S(11)	86.2(2)
S(2)−V(1)−S(6)	140.0(2)	S(8)−V(3)−S(12)	149.0(2)
S(2)−V(1)−O(1)	111.0(6)	S(8)−V(3)−O(3)	106.1(5)
S(5)−V(1)−S(6)	69.9(2)	S(11)−V(3)−S(12)	70.2(2)
S(5)−V(1)−O(1)	103.3(5)	S(11)−V(3)−O(3)	106.5(4)
S(6)−V(1)−O(1)	105.4(5)	S(12)−V(3)−O(3)	99.8(4)
S(1)−V(2)−S(2)	100.0(2)	S(7)−V(4)−S(8)	99.3(2)
S(1)−V(2)−S(3)	136.0(3)	S(7)−V(4)−S(9)	85.3(2)
S(1)−V(2)−S(4)	86.3(2)	S(7)−V(4)−S(10)	145.4(3)
S(1)−V(2)−O(2)	110.3(6)	S(7)−V(4)−O(4)	106.6(4)
S(2)−V(2)−S(3)	84.7(2)	S(8)−V(4)−S(9)	140.8(3)
S(2)−V(2)−S(4)	149.0(2)	S(8)−V(4)−S(10)	85.9(2)
S(2)−V(2)−O(2)	106.8(6)	S(8)−V(4)−O(4)	109.1(4)
S(3)−V(2)−S(4)	70.4(2)	S(9)−V(4)−S(10)	70.3(2)
S(3)−V(2)−O(2)	110.0(5)	S(9)−V(4)−O(4)	106.7(4)
S(4)−V(2)−O(2)	99.2(4)	S(10)−V(4)−O(4)	103.8(4)
V(1)−S(1)−V(2)	75.2(2)	V(3)−S(7)−V(4)	76.0(1)
V(1)−S(2)−V(2)	75.1(2)	V(3)−S(8)−V(4)	76.9(1)

Table 7. Comparison of Structural Parameters of the $[V_2O_2(\mu\text{-}S)_2(Et_2dtc)_2]^{2-}$ Moieties in $[Et_4N]_3Na[\mathbf{3}]_2$ and $[Et_4N]\mathbf{4}$

	3	**4**[32]
V−V (Å)	2.781(4)−2.813(3) mean[a] 2.797(16)	2.718(1)
V═O (Å)	1.61(2)−1.63(1) mean[a] 1.62(1)	1.676(4)−1.677(4) mean[a] 1.677(1)
V−S_b (Å)	2.258(5)−2.294(6) mean[a] 2.277(4)	2.231(2)−2.264(2) mean[a] 2.251(7)
V−S_{dtc} (Å)	2.438(6)−2.497(5) mean[a] 2.472(6)	2.420(1)−2.454(3) mean[a] 2.432(7)
O−V−S (deg)	99.8(4)−110.3(6) mean[a] 106.4(8)	102.0(1)−114.8(2) mean[a] 106.5(13)
S_{dtc}−V−S_{dtc} (deg)	69.9(2)−70.4(2) mean[a] 70.2(1)	71.03(7)−71.67(7) mean[a] 71.32(29)
S_b−V−S_b (deg)	99.3(2)−100.4(2) mean[a] 99.95(23)	99.06(5)−99.48(6) mean[a] 99.27(21)

[a] Number in parentheses represents the standard deviation from the mean, $\sigma = [\sum_{i=1}^{N}(x_i - \bar{x})^2/N(N-1)]^{1/2}$.

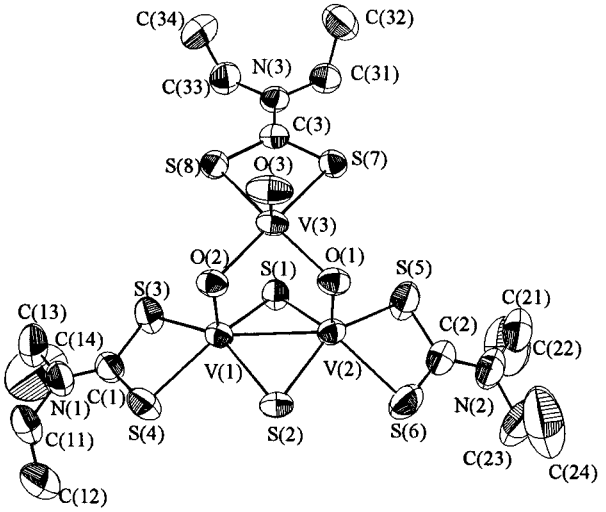

Figure 4. Structure and labeling of $[V_3O_3(\mu\text{-}S)_2(Et_2dtc)_3]^-$. Thermal ellipsoids are drawn by ORTEP at 30% probability.

The hydrogen bonding of the solvent molecules CH_3OH (O(5) is contained) and H_2O to the oxygen atoms of the **3** anions was not observed, since the shortest O···O distance of 3.21(3) Å (O(4)···O(5)) was found to be outside of the normal H-bonding range of 2.40−2.90 Å for O−H···O.[39] Also, the shortest O···Na distance for the solvent molecules is 3.90(3) Å (O(5)···Na(2)), being greater than the van der Waals distances.

Spectral Features. Infrared Spectra. A strong absorption in the region 340−370 cm^{-1} was observed for each complex obtained in this work, to be assigned to the V−S_{dtc} vibration.[40] In the range of 400∼500 cm^{-1} where ν(M−S_b) frequencies are expected,[41] $V_2Ag_{1-2}S_4$ cubanelike clusters exhibit a shoulder at 455 cm^{-1} for **1** and widening peaks at 430 and 470 cm^{-1} for **2** corresponding to V−μ_{2-3}-S vibrations in the cuboidal core. For **3** and **4** which contain the $V_2(\mu\text{-}S)_2$ unit, the V−S_b vibrations appear at 467 cm^{-1} for **3** and 450 and 487 cm^{-1} for **4**. The most pertinent difference between the $V_2Ag_{1-2}S_4$ cubanes (**1** and **2**) and oxovanadium cluster anions (**3** and **4**) is the presence of the V═O stretch in the range 844−970 cm^{-1} in the latter complexes. The frequencies are consistent with the range reported for a large set of oxovanadium complexes.[42] **4** contains two sets of V═O bonds[7a,32] of which the V═O of 1.589(5) Å is normal corresponding to the stretching frequency at 970 cm^{-1}, while the other set of 1.677(1) Å is additionally coordinated to $VO(Et_2dtc)^+$ and is responsible to the lowest frequency of 844 cm^{-1} in Table 8. **3** contains V═O bonds of 1.61(2)−1.63(1) Å exhibiting a frequency at 939 cm^{-1}. It is noted that the additional coordination of V═O to Na^+ may be a reason for the lengthening of the V═O bonds to ca. 1.62 Å, being greater than the normal value (1.58−1.60 Å). The variation of the frequency for some square pyramid vanadyl(IV) complexes in Table 8 could be considered to be occurring from the additional coordination of another metal cation (such as Na^+ in **3**, $[VO(edt)_2]^{2-}$, and $[VO(mp)_2]^{2-}$; V^{4+} in **4**) which weakens the V═O bond to give rise to the red shift of the infrared frequency. Other infrared bands associated with the anions **1**−**4** are the following: ν(P−C),[43] 492 cm^{-1} (**1** and **2**); ν(C═S),[40] 980 (**1**), 1000 (**2**), 999 (**3**), and 996 cm^{-1} (**4**); ν(C═N, R_2dtc),[40] 1510 (**1**), 1489 (**3**), and 1492 cm^{-1} (**4**).

Table 8. Comparison of V═O Stretching Frequency Data for V/S(O) Complexes

compd	V═O (Å)	$\nu_{V=O}$ (cm^{-1})	ref
$[V_2O_2S_2(Et_2dtc)_2]^{2-}$	1.62(1)[a]	939	this work
$[V_3O_3S_2(Et_2dtc)_3]^-$	1.589(5)	970	7a
	1.677(1)[b]	912	
$[VO(mp)_2]^{2-}$ [c]	1.611(5)[a]	940	11
$[VO(edt)_2]^{2-}$ [d]	1.625(2)[a]	930	37
VO(salpn)[e]	1.633(9)[b]	854	44
$[VO(2\text{-}SC_5H_4NO)_2]$	1.593(3)	984	45, 46
$VO(Et_2dtc)_2$	1.591(4)	970	47
VO(tsalen)[f]	1.598(6)	975	48

[a] The V═O coordinates to Na^+ in the complex. [b] Complex contains V═O−V links. [c] mp = 2-mercaptophenolato. [d] edt = ethane-1,2-dithiolato. [e] [*N*,*N*′-Propylenebis(salicylideneaminato)]oxovanadium(IV). [f] [*N*,*N*′-Ethylenebis(thiosalicylideneaminato)]oxovanadium(IV).

NMR Spectra. Characteristic ^{1}H NMR resonances and their contribution for the ligands and cations are summarized in the Experimental Section. The spectrum of $[Et_4N]_2\mathbf{2}$ is rather simple only showing the ^{1}H signals of Et_4N^+ and PPh_3 at 1.16 and 3.22 ppm for the former and in the range of 7.56−7.69 ppm for the latter, of which the intensity ratio of absorptions at 7.61−7.62, 7.56−7.57, and 7.64−7.69 ppm is 1:2:2 indicating that the chemical shift of *p*-H is between those of *m*-H and *o*-H. Its ^{13}C NMR spectrum shows the resonances of the PPh_3 ligand as four main peaks (128.9, 131.9, 132.4, and 133.1 ppm) of which the resonances with low intensity at 132.4 and 133.1 ppm downfield are assigned to the contribution of *p*-C and P−C, respectively, while the resonances at 128.9 and 131.9 ppm are assigned to *m*-C and *o*-C, respectively. Two sets of ^{31}P resonances (Figure 5a) with equal intensity are preferably considered to be occurring from ^{31}P−^{107}Ag coupling (J = 527.4 Hz), though there are two ligating PPh_3 ligands existing in the structure. Since each resonance is very broad with a line width of 72 Hz at half-height and contains two distinguishable signals (16.6, 16.8 and 19.1, 19.3 ppm), it may well hide two V atoms in a similar environment. A broad resonance at 231 ppm was observed in the ^{51}V NMR (Figure 5b) of $[Et_4N]_2\mathbf{2}$, which is believed to be responsible for the $V^{IV}(\mu\text{-}S)_2V^{IV}$ moiety with a V−V single bond and may also be an indication of the two V

(39) Wells, A. F. *Structural Inorganic Chemistry*, 5th ed.; Clarendon Press: Oxford, U.K., 1984.
(40) Bradkey, D. C.; Gitlitz, M. H. *J. Chem. Soc. A* **1969**, 1152.
(41) Müller, A.; Jaegermann, W.; Helmann, W. *J. Mol. Struct.* **1983**, *100*, 559.
(42) (a) Selbin, J. *Coord. Chem. Rev.* **1966**, *1*, 293. (b) Selbin, J. *Chem. Rev.* **1965**, *65*, 153.
(43) *Sadtler Infrared Standard Grating Spectra*; Sadtler Research Laboratory: Philadelphia, PA, 1975; Vol. 35.

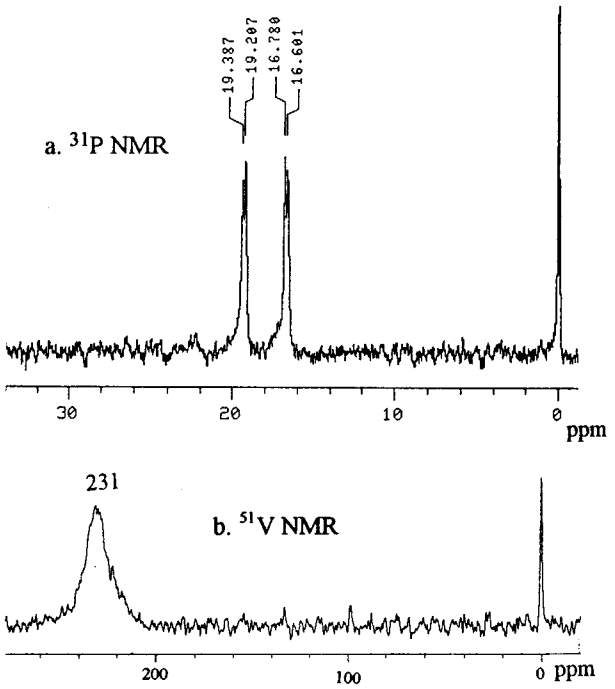

Figure 5. ^{31}P NMR (a) and ^{51}V NMR (b) spectra of $(Et_4N)_2[V_2Ag_2S_4(CS_3)_2(PPh_3)_2]$ in DMSO solution at ambient temperature.

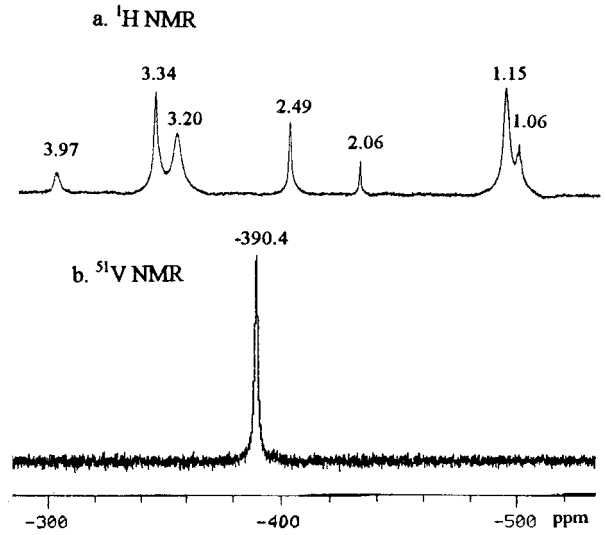

Figure 6. ^{1}H NMR and ^{51}V NMR spectra of $(Et_4N)_3Na[V_2O_2(\mu\text{-}S)_2(Et_2dtc)_2]_2$ in DMSO-d_6 solution at ambient temperature: (a) ^{1}H NMR, δ 1.06 (CH_3, Et_2dtc), 1.15 (CH_3, Et_4N^+), 2.06 (CH_3CN), 2.49 (DMSO), 3.20 (CH_2, Et_4N^+), 3.34 (H_2O), 3.97 (CH_2, Et_2dtc) ppm; (b) ^{51}V NMR.

atoms being in a similar environment. A comparable example is $[V_2(S_2)_2(CS_3)_4]$,[4-38] which shows its sharp ^{51}V resonance at 125 ppm in DMSO/CD_3CN. It is obvious that V^{IV} nuclei in complex $[Et_4N]_2$**2** are less effectively shielded by five S atoms than those of $[V_2(S_2)_2(CS_3)_4]^{4-}$ shielded by eight S atoms, giving rise to the ^{51}V signal downfield.

The ^{1}H NMR spectrum (Figure 6a) of $[Et_4N]_3Na[V_2O_2S_2(Et_2dtc)_2]_2$ in DMSO-d_6 shows a broad peak at 3.97 ppm which is close to the chemical shift (4.0 ppm) of α-H (CH_2) in Et_2dtcNa and can be reasonably assigned to CH_2 resonances of Et_2dtc ligands chelating to the $V^{IV}(\mu\text{-}S)_2V^{IV}$ structural unit, since d^1-d^1 electrons are spin paired leading to a diamagnetic result. Interestingly, in CD_3CN solution, the ^{1}H NMR spectrum of the complex shows somewhat of a difference from that in DMSO-

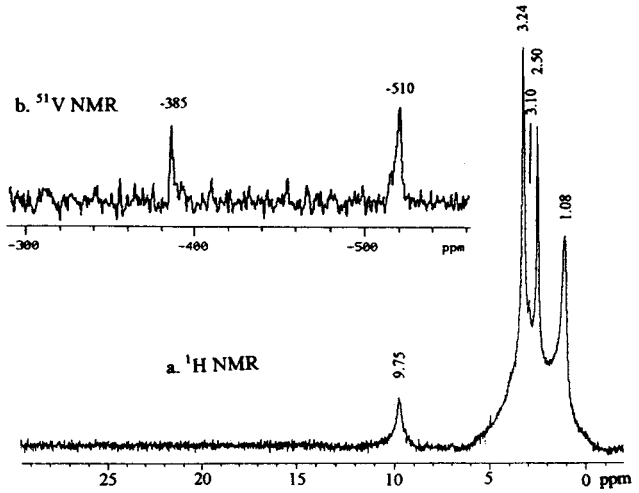

Figure 7. ^{1}H NMR and ^{51}V NMR spectra of $(Et_4N)[V_3O_3(\mu\text{-}S)_2(Et_2dtc)_3]$ in DMSO-d_6 at ambient temperature: (a) ^{1}H NMR, δ 1.08 (CH_3, Et_4N^+ and Et_2dtc), 2.50 (DMSO), 3.10 (CH_2, Et_4N^+), 3.24 (H_2O), 9.75 (CH_2, Et_2dtcVO) ppm; (b) ^{51}V NMR, δ −385 ($[V_2O_2S_2(Et_2dtc)_2]$), −510 ($VO(Et_2dtc)$) ppm.

d_6: several sets of broad peaks at 3.90 and 4.10 ppm were observed and can also be assigned to the CH_2 resonances of Et_2dtcV. However, the complicated structural feature resulting from the coordination of the alkali ion would give rise to the obvious widening and the occurrence of these sets of signals around 4.0 ppm, if we consider that the complex may retain the Na−O contacts in a weak polar solvent CD_3CN, while in DMSO-d_6, a relatively strong polar solvent, they would be totally dissociated to form free $[V_2O_2(\mu\text{-}S)_2(Et_2dtc)_2]^{2-}$ anions. It is noted that **4** shows a broad signal at 9.75 ppm in DMSO-d_6 as shown in Figure 7a. This paramagnetic chemical shift is tentatively assigned to the contribution of α-H in the Et_2dtc ligand chelating to the paramagnetic V^{IV} atom and is comparable to that of complex $[V_3S_7(Me_2dtc)_3]^-$ (δ 10.67 and 8.72 ppm).[19] Paramagnetism of the V^{IV} center in $V_3O(\mu\text{-}O)_2(\mu\text{-}S)_2$ core has been pointed out by ESR study in the literature[7a] though the NMR research was not reported. The intensity ratio of the absorptions at 9.75 and 1.08 ppm (CH_3, β-H in Et_4N^+ and Et_2-dtc ligands) is 1:6 which is near the ratio of the α-H (CH_2) amount in the fragment of the paramagnetic V center to that of β-H (CH_3) in both the ligand and the cation Et_4N^+. However, the resonance of the methylene in the $[V_2O_2(\mu\text{-}S)_2(Et_2dtc)_2]^{2-}$ fragment is obscured in the spectrum causing some uncertainty. The interesting difference of ^{51}V NMR spectra (Figure 6b and 7b) between **3** and **4** has been noted: the spectra of **3** exhibit a sharp peak at −390 ppm (DMSO-d_6) and −394 ppm (CD_3CN) supporting that only one kind of vanadium center exists in the complex and that there is strong coupling between the two V^{IV} atoms, while **4** exhibits two somewhat broad signals at −519 and −385 ppm in DMF. This difference confirms that there are two types of vanadium centers in the structure of **4**, i.e., paramagnetic V^{IV} center and the coupling V^{IV} centers in the $V^{IV}(\mu\text{-}S)_2V^{IV}$ unit, and that the latter is responsible for the resonance at the range of −385 to −394 ppm, though the peak of **4** is obviously broad because of the existence of the paramagnetic V^{IV} center. Compared to the ^{51}V resonance of **2**, the upfield shifts for **3** and **4** may stem from the oxo−V_2S_2 unit which is different from the sulfide−V_2S_2 unit of **2**, since the oxovanadium complex usually has the ^{51}V resonance upfield[38,49] when compared to the corresponding vanadium

Table 9. Comparison of ^{51}V NMR Data for Some V/S(O) Complexes

compd	oxidn state of V	δ (ppm)	solvent	ref
VS_4^{3-}	5+	1388	DMSO	50
$VS_2(\eta\text{-}S_2)(SPh)^{2-}$	5+	930	DMSO	38
$[VS_4Cu_4(PhS)_4]^{3-}$	5+	670	DMSO	25
$[VS_4Cu_4(OC_4H_8dtc)_2(PhS)_2]^{3-}$	5+	663	DMSO	25
$[V_2Ag_2S_4(CS_3)_2(PPh_3)_2]^{2-}$	4+	231	DMSO	*a*
$[V_2(S_2)_2(CS_3)_4]^{4-}$	4+	125	DMSO/CD_3CN	38
$V_2(S_2)_2(Et_2dtc)_4$	4+	103	$CDCl_3$	38
$[V_2O_2S_2(Et_2dtc)_2]^{2-}$	4+	−394	CH_3CN	*a*
		−390	DMSO	
$[V_3O_3S_2(Et_2dtc)_3]^{-}$	4+	−385	DMSO	*a*
		−519		

[a] This work.

sulfide complex. Table 9 gives ^{51}V NMR data for some V complexes with various oxidation states the vanadium and S/O coordination spheres, exhibiting some general rules of the ^{51}V NMR spectra as follows: (1) The vanadium oxide complex has an upfield signal in comparison with the corresponding vanadium sulfide complex, since the S ligand gives rise to low shielding.[38] (2) Spin pairing of the d^1-d^1 electrons leads to diamagnetic results (such as the sharp ^{51}V signal) for the dinuclear V^{IV} complexes, while shielding of the d^1 electron gives rise to the ^{51}V signal upfield of the V^{IV} complex compared to that of the V^V complex. (3) In the hetero- and polymetallic V cluster anions **2** and **4**, coupling between the two paramagnetic V centers of the $V_2(\mu\text{-}S)_2$ unit would be affected by the other metal centers Ag^I and V^{IV}, leading to the broad ^{51}V signals (Figures 5b and 7b). Also, the relatively broad ^{51}V signal has been observed in the spectrum[25] of $[VS_4Cu_4(PhS)_4]^{3-}$ compared to those of the other V^V/S complexes[38,50] listed in Table 9, indicating the influence of Cu^I on the V^V nucleus.

Cyclic Voltammetry. Cyclic voltammetry (Figure 8a) of the trinuclear V_3 anion **4** in DMF shows a series of redox processes of which reductions at −0.77 and −1.15 V on the cathodic scan and oxidations at −0.65, +0.15, and +0.77 V on the return scan were observed. Interestingly, the dinuclear anion **3** shows some electrochemical features (Figure 8b) similar to those of **4**: a couple at −0.73 V/−0.65 V and oxidation peaks at +0.1 and +0.65 V at the same determination conditions. According to the structures of **3** and **4** and the NMR data, we consider that the V_3 trimer undergoes dissociation in the electrochemical process to form the dinuclear fragment $[V_2O_2(\mu\text{-}S)_2(Et_2dtc)_2]^{2-}$ and mononuclear fragment $[VO(Et_2dtc)(DMF)_2]^{+}$. The couple

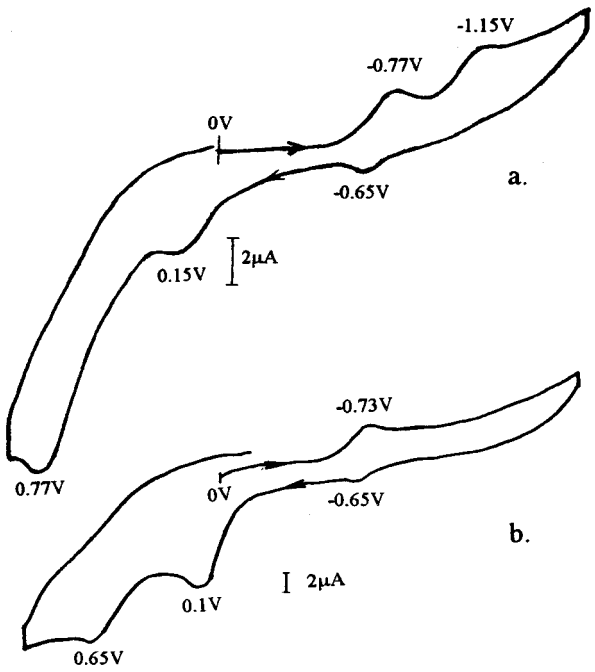

Figure 8. Cyclic voltammograms of complexes of **3** (a) and **4** (b) in DMF solution in the range of −1.0 to 1.5 V at ambient temperature.

at −0.77 V/−0.65 V is believed to be due to the redox of V^{IV}/V^{III} in the equation

$$[V_2O_2S_2(Et_2dtc)_2]^{2-} \underset{-0.65\ V}{\overset{-0.77\ V}{\rightleftharpoons}} [V_2O_2S_2(Et_2dtc)_2]^{3-}$$

and is identified by the same couple at −0.7 V/−0.65 V for **3** in DMF. The cathodic peak at −1.15 V for **4** may arise from the mononuclear fragment $[VO(Et_2dtc)(DMF)_2]^{+}$, since $VO(Et_2dtc)_2$ was reported to have a reduction at −1.35 V[35] in CH_3CN. The anodic peaks at +0.15 V for **4** and at +0.1 V for **3** appear to be related to the oxidation of the ligand coordinated to vanadium when compared to the oxidation of free ligand Et_2dtcNa at +0.05 V. Finally, the common oxidation peak for both **3** and **4** at +0.77 to +0.65 V is supposed to be due to the following irreversible oxidation of the dinuclear fragment:

$$[V_2O_2S_2(Et_2dtc)_2]^{2-} \xrightarrow{0.6-0.77\ V} [V_2O_2S_2(Et_2dtc)_2]^{-}$$

Though the aforementioned discussions of structures, spectra, and electrochemistry support the existence of the $V_2Y_2(\mu\text{-}S)_2$ (Y = O, S) intermediate, it is still important to separate the intermediates, especially $V_2S_2(\mu\text{-}S)_2$, from the reaction system and to study their chemical reactions, so that we can obtain direct evidence of the aggregation mechanism. Currently, this is the focus of our attention.

Acknowledgment. This work was supported by funding from the National Science Foundation of China.

Supporting Information Available: Tables of crystallographic data, atomic coordinates and *B* values, bond lengths and angles, and anisotropic thermal parameters for the complexes containing the **1**−**3** anions (22 pages). Ordering information is given on any current masthead page.

IC9715310

(44) Mathew, M.; Carty, A. J.; Palenik, G. J. *J. Am. Chem. Soc.* **1970**, *92*, 3197.
(45) Higes-Rolando, F. J.; Perez-Florindo, A.; Valenzuela-Calahorro, C.; Martin-Ramos, J. D.; Romero-Garzon, J. *Acta Crystallogr.* **1994**, *C50*, 1049.
(46) Tsagkalidis, W.; Rodewald, D.; Vergopoulos, V. *Inorg. Chim. Acta* **1994**, *219*, 213.
(47) Henrick, K.; Raston, C. L.; White, A. H. *J. Chem. Soc., Dalton Trans.* **1976**, 26.
(48) Dutton, J. C.; Fallon, G. D.; Murray, K. S. *Inorg. Chem.* **1988**, *27*, 34.
(49) Howarth, O. W. *Prog. NMR Spectrosc.* **1990**, *22*, 453.
(50) (a) Harrison, T.; Howarth, O. W. *J. Chem. Soc., Dalton Trans.* **1986**, 1405. (b) Zhang, Y.; Holm, R. H. *Inorg. Chem.* **1988**, *27*, 3875.